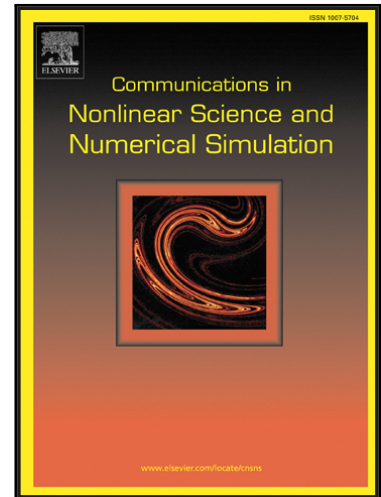


Accepted Manuscript

The complexity of intracranial pressure as an indicator of cerebral autoregulation

Nicolás Ciarrocchi, Nicolás Quiróz, Francisco Traversaro, Eduardo San Roman, Marcelo Risk, Fernando Goldemberg, Francisco Redelico

PII: S1007-5704(19)30086-3
DOI: <https://doi.org/10.1016/j.cnsns.2019.03.018>
Reference: CNSNS 4802



To appear in: *Communications in Nonlinear Science and Numerical Simulation*

Received date: 20 August 2018
Revised date: 12 March 2019
Accepted date: 17 March 2019

Please cite this article as: Nicolás Ciarrocchi, Nicolás Quiróz, Francisco Traversaro, Eduardo San Roman, Marcelo Risk, Fernando Goldemberg, Francisco Redelico, The complexity of intracranial pressure as an indicator of cerebral autoregulation, *Communications in Nonlinear Science and Numerical Simulation* (2019), doi: <https://doi.org/10.1016/j.cnsns.2019.03.018>

This is a PDF file of an unedited manuscript that has been accepted for publication. As a service to our customers we are providing this early version of the manuscript. The manuscript will undergo copyediting, typesetting, and review of the resulting proof before it is published in its final form. Please note that during the production process errors may be discovered which could affect the content, and all legal disclaimers that apply to the journal pertain.

Highlights

- Loss of complexity is associated with elevated Intracranial Pressure
- The loss of compensatory mechanism in the cerebral autorregulation increases the Missing Patterns in the Permutation Entropy calculation

ACCEPTED MANUSCRIPT

The complexity of intracranial pressure as an indicator of cerebral autoregulation

Nicolás Ciarrocchi^a, Nicolás Quiróz^b, Francisco Traversaro^{b,c}, Eduardo San Roman^a, Marcelo Risk^b, Fernando Goldemberg^d, Francisco Redelico^{b,f}

^a *Hospital Italiano de Buenos Aires, Servicio de Terapia Intensiva Adultos, Perón 4190 - (C1199ABB) Ciudad Autónoma de Buenos Aires, Argentina.*

^b *Instituto de Medicina Traslacional e Ingeniería Biomedica, UE de triple dependencia CONICET - Instituto Universitario del Hospital Italiano (IUHI) - Hospital Italiano (HIBA), Potosí 4239 - (C1199ABB) Ciudad Autónoma de Buenos Aires, Argentina.*

^c *Facultad de Ciencias Agrarias e Ingeniería, Universidad Católica Argentina (UCA)*

^d *The University of Chicago Medicine 5841 S. Maryland Avenue, MC 2030 Chicago, IL 60637.*

^e *CONICET - Hospital Italiano de Buenos Aires, Departamento de Informática en Salud, Perón 4190 - (C1199ABB) Ciudad Autónoma de Buenos Aires, Argentina.*

^f *Universidad Nacional de Quilmes - Departamento de Ciencia y Tecnología, Roque Sáenz Peña 352 (B1876BXD), Bernal Buenos Aires, Argentina.*

Abstract

Intracranial Pressure (ICP) is one of the main neuromonitors used today to guide the treatment of acute neurological patients in the Intensive Care Unit (ICU).

Within this article the complexity of periods of intracranial hypertension is evaluated and compared with periods of stable intracranial tension. Using the multiparameter intelligent monitoring in intensive care III (MIMIC-III) database from the *Beth Israel Deaconess Medical Center* the complexity of periods of stable intracranial tension and high intracranial hypertension are evaluated using two quantifiers: the Permutation Entropy and their respective number of missing patterns. Both indicate a loss of complexity in hypertension signals. A physiological explanation of this loss of complexity is given using a dynamical model of the Cerebral Autoregulation and Cerebral Hemodynamics.

Keywords: Intracranial Pressure, Clinical manifestation of Complexity, Permutation Entropy

1 Introduction

2 Intracranial Pressure (ICP) is one of the main neuromonitories used to-
3 day to guide the treatment of acute neurological patients in the Intensive
4 Care Unit (ICU) [1]. It is determined by the relation of the cranial cavity
5 and its content (brain tissue, cerebrospinal fluid and blood volume) and reg-
6 ulated by a complex mechanism that allows to maintain its value in different
7 situations [2]. One component of this mechanism is Cerebral Autoregulation
8 (CA) that enables changes in blood flow and volume in the face of changes in
9 blood pressure. CA and ICP have a complex interrelation where the main-
10 tenance of ICP depends on the preservation of CA and this depends in turn
11 on ICP since the presence of intracranial hypertension (ICH) exhausts CA
12 mechanism. Many mathematical models were proposed to understand the
13 CA dynamics [3, 4, 5]. From a system's dynamics point of view and fol-
14 lowing the model proposed by Ursino *et al.* [5] for the interaction between
15 ICP and cerebral hemodynamics (Fig. 1), there are three different negative
16 feedback control loops that preserve cerebral autoregulation, and a positive
17 feedback loop that causes instabilities due to active changes in the arterial-
18 arteriolar blood volume. The instability in CA caused by the feedback IV
19 (See Fig. 1) is the type of instability studied in this article using a com-
20 plexity framework: if the patient has a modest Cerebrospinal Fluid (CSF)
21 outflow resistance and an a low intracranial compliance, this triggers a cycle
22 of positive feedback where, as intracranial compliance worsens, the positive
23 feedback cycle becomes more influential in intracranial dynamics, moving the
24 system away from optimal equilibrium, analogue to Rosner's vasodilatatory
25 cascade. When the pressure in cerebral perfusion decreases, it also generates
26 a decrease in the Cerebral Blood Flow (CBF) with the consequent vasodi-
27 lation effect to maintain a constant flow, leading to an increase in Cerebral
28 Blood Volume (CBV), thus increasing the ICP, which causes a greater de-
29 crease in Cerebral Perfusion Pressure (CPP) generating a vicious circle, i.e.
30 positive feedback. The other three feedbacks are escape ways that try to
31 hold the ICP in normal values.

32 The study of the complexity in physiological systems begins with the work
33 by Kaplan *et al.* [6]. In that article the difference between the complex-
34 ity of the heart rate frequency between a group of young patients (21-35
35 years) and adult patients (62-90 years) was quantified, finding a reduction
36 in the complexity of the former with respect to the latter. The hypothe-
37 sis of reduction in the complexity of physiological systems with respect to

38 age and disease was postulated by Lipsitz and Goldenberg [7]. Since then,
39 there have been many published articles supporting this hypothesis, in such
40 different subjects as *Epilepsy* [8, 9], *Congestive Heart Failure* [10], *Dilated*
41 *Cardiomyopathy* [11], *Subarachnoid Hemorrhage* [12], among others. While
42 there are many working definitions about complexity [13], within this arti-
43 cle we adopt a definition of structural complexity, following the taxonomy
44 proposed by Tang *et al.* [14], using a global quantifier: the Permutation
45 Entropy (PE) proposed by Bandt and Pompe in [15]. The PE is an informa-
46 tional quantifier [16] that takes into account the time correlation structure of
47 the signal. Its computation is fast, requires not too long time series [17], it
48 is robust against noise [18] and distributional assumptions of the time series
49 [19]. PE was previously used as an useful complexity tool in neuroscience in
50 several papers: *Epilepsy* ([19, 20]), *Anesthesia* ([21, 22, 23, 24, 25, 26]), and
51 *Cognitive Neuroscience* ([27, 28, 29]), however we have not found its use in
52 the analysis of signals in intensive care patients.

53 PE measures the degree of expectation in the correlation structure of a time
54 series, *so high values of PE indicate high unpredictability and therefore high*
55 *structural-global complexity*. Although in Section 1 we present a synthesis of
56 the calculation of PE we refer to [8, 15, 17] for a more detailed study on this
57 quantifier and its relationship with complexity. For all of this, within this
58 article complexity and PE are equivalent. Due the interaction of the four
59 loops in Fig. 1, the attractor of the ICP dynamics is a fixed point hence the
60 direction of the change of the complexity in the presence of a pathology is
61 expected to be negative, and in fact it happens.

62

63 1. Materials and Methods

64 This a retrospective analysis using the multiparameter intelligent moni-
65 toring in intensive care III (MIMIC-III) which is a large publicly available
66 database comprising de-identified health-related data associated with over
67 40000 patients in critical care units at the *Beth Israel Deaconess Medical*
68 *Center* (BIDMC) between 2001 and 2012 [30, 31]. The MIMIC-III Waveform
69 Database Matched Subset (<http://physionet.org/physiobank/database/mimic3wdb/matched/>)
70 contains all MIMIC-III waveform records that have been associated to MIMIC-
71 III Clinical Database records containing 22317 waveform records and 22247
72 numeric records matched with 10282 clinical data [32, 30] Despite the large
73 number of patients registered at the MIMIC-III Waveform Database Matched

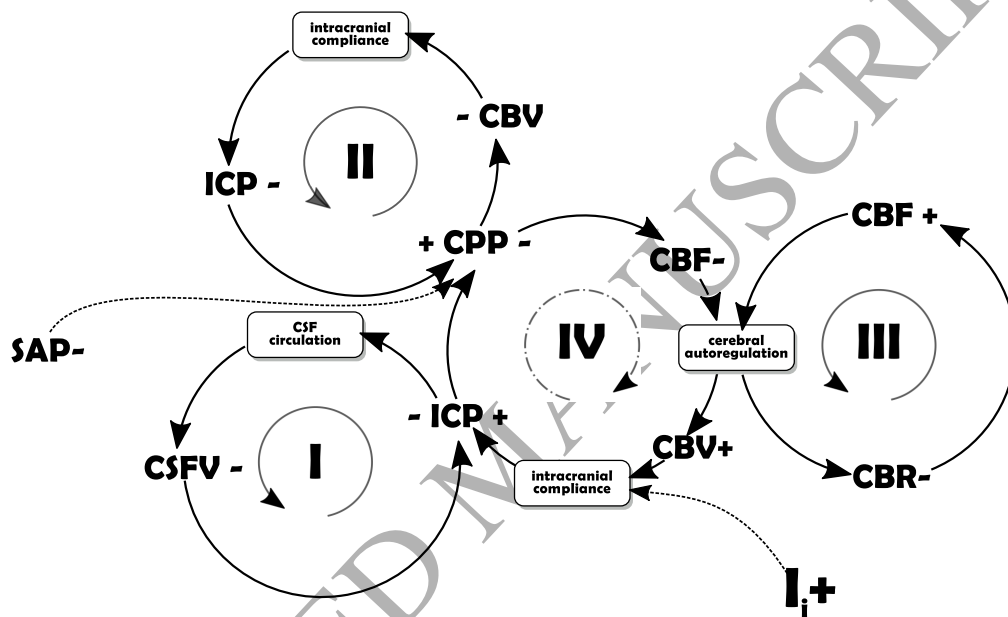


Figure 1: The interaction between Intracranial Pressure and cerebral hemodynamics. There are three different negative feedback control loops that preserve cerebral self-regulation; *feedback I: the cerebrospinal fluid (CSF) loop*, *feedback II: when a diminution of the Systemic Arterial Pressure is present, the Cerebral Perfusion Pressure (CPP) also decreases, generating the decreases of the Cerebral Blood Volume (CBV) that induces, via the intracranial compliance, a reduction of the intracranial pressure (ICP), and the effect of self-regulation in Cerebral Blood Flow (CBF) (feedback III), thus increasing the ICP, which leads to greater decrease in CPP generating a positive feedback (feedback IV).*

74 Subset, only a small fraction corresponds to patients with acute neurological
75 disease (see Table I) whose records contain ICP signal measurements. They
76 account for a total of 37 days of ICP signals measured at a 125 Hz sample
77 rate (15 GB of signal data). Both physiological and clinical data were down-
78 loaded following the recommendations in [33, 30, 32, 34, 35]. In order to have
79 access to the MIMIC-III Clinical Database, the completion of a CITI Data
80 or Specimens Only Research course was required as well as the creation of an
81 account at PhysioNet. (<https://www.citiprogram.org/verify/?k8e6410f7-6dbc-41d8-ae12-9b29f7b6372f-24580999>).
82

83
84 Each physiological signal data is composed of a list of waveform segments.
85 These segments were independently processed. In order to get complete
86 and free of artifact signals an imputation method was applied to estimate
87 for both missing values (NA) and out of range data in each signal. The
88 imputed value is the mean of the 10 nearest neighbors of the patient's signal
89 missing value. Next, in order to avoid the pulsation effect of respiration and
90 heartbeat, a moving average filter was applied with a sliding window of 10
91 seconds span and a maximum overlap [36]. The segments may or may not
92 contain episodes of Intracranial Hypertension (ICH), defined as $ICP \geq 20$
93 mmHg during a period of 5 min. Following this criteria, an autonomous
94 episode detector was developed to identify ICH criteria in all segments. The
95 resultant episode subsets were visually examined and either confirmed or
96 rejected (i.e. artifacts in recordings). Finally, each accepted episodes can
97 be divided into three adjacent non-overlapping segments with the following
98 characteristics: A maximum 300 s stable zone (ST), a 10 - 240 s transition
99 zone (TZ), and at maximum 20 s critical zone (CR). We used three criteria
100 to identify acute episodes of ICH: the difference between the minimum value
101 in the critical region and the maximum value in the stable region must be at
102 least 5 mmHg, the minimum value in the CR must be greater than 20 mmHg;
103 and the maximum value in the ST must be less than 20 mmHg [37]. The
104 original ICP signal for patient 87969 and the corresponding filtered signal
105 as well as an schematic representation of both the ICH and all regions are
106 showed in Fig. 2, based in [38, 39]. These criteria were applied to get two
107 non-overlapped signals, i.e. the ST and CR zones, to quantify the loss of
108 complexity between them.

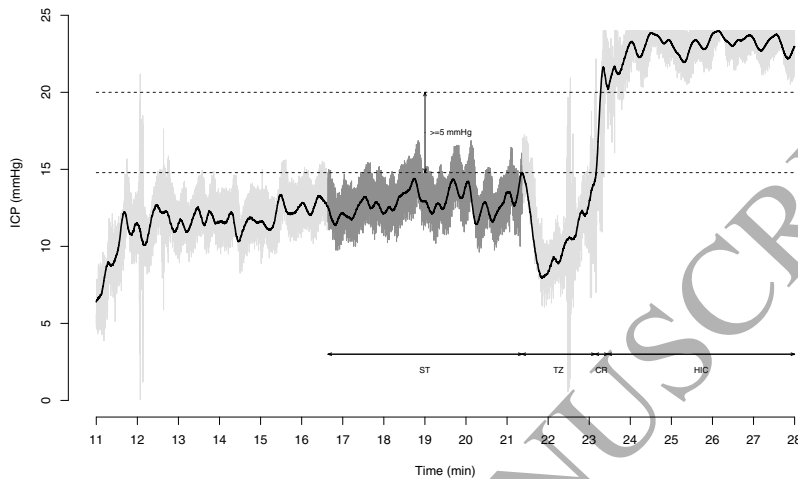


Figure 2: ICP signal for the third ICH episode detected in segment 368853 corresponding to patient 87969. The light gray is the actual 18 min long ICP signal sampled at 125 Hz, the dark line is the 10 s moving average for the same signal.

109 1.1. Permutation Entropy

110 One measure for complexity is named Entropy, which is defined as a
 111 quantifier of the uncertainty present in a system. One of the most well
 112 accepted formula is named Shannon Entropy since Claude Shannon [40], and
 113 it is defined as:

$$\mathcal{H} = \left\{ - \sum_{i=1}^{m!} P(\pi_i) \ln(P(\pi_i)) \right\} / S_{max}, \quad (1)$$

114 where $P(\pi_i)$ represents the probability that the system belongs the state
 115 π_i and S_{max} is the Shannon Entropy for the equilibrium state. In our case the
 116 system under study is the cerebral autoregulation through the intracranial
 117 pressure signal obtained from a given patient and the $P(\pi_i)$ are calculated
 118 by the evolution of that signal embedded in a m-dimensional vector. When
 119 the probabilities $P(\pi_i)$ are calculated by the probability of occurrence of cer-
 120 tain patterns derived from Bandt and Pompe methodology of symbolization
 121 [15] it is called Permutation Entropy (PE) . One important concept derived
 122 from PE is the number of missing patterns (NMP) defined as the number of

123 patterns that the m -dimensional vector never arise. The reader interested in
 124 mathematical details will find a brief discussion in Fig. 3, Appendix I and
 125 in [15, 8]

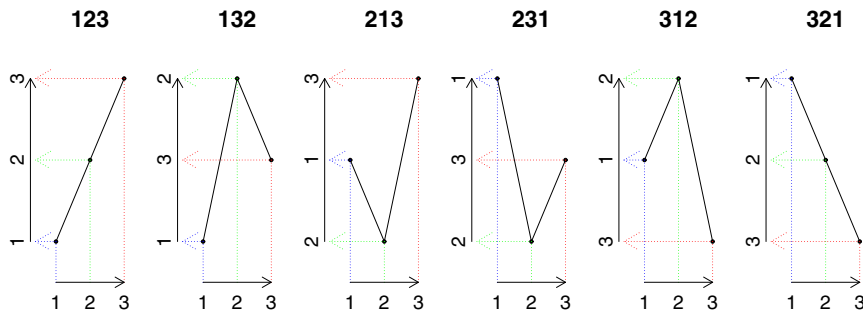


Figure 3: Symbols of the Bandt and Pompe symbolization for $m = 3$. This methodology simply maps each value x_i in the 3-dimensional vector $X_m(t)$ ordering its index $t \in \{1, 2, \dots, m\}$ according to the increasing amplitude (rank) of each x_i in $X_m(t)$. It can be seen that the indexes of the time axis are fixed in chronological order, and they are mapped onto the vertical (amplitude) axis. For each pattern $X_3(t) = (x_t, x_{t+1}, x_{t+2})$, the resultant symbol π_i can be obtained reading the labels in the vertical axis from the bottom to the top (in the direction of the increasing amplitude).

126

127 2. Results

128 Twelve patients were analyzed looking for ICH and stable regions. As it
 129 is shown in Table 1 there were 9 females and 3 males with an age with a range
 130 from 32 to 82 years old and a mean of 56.9 ± 14.8 years old, the length of the
 131 stay in the ICU was from 9 to 82 days; six patients present subarachnoid
 132 hemorrhage and six patient, intracranial hemorrhage. Only 4 patients present
 133 ICH periods as defined in material and methods, three patients present only
 134 one ICH each one and one patient present four, leading to 7 signals of ICH,
 135 see Table 2.

136 *Permutation Entropy* was estimated for all patients for their respective
 137 Stable and Intracranial Hypertension, segment 3629298 does not has a Stable
 138 region. Across all segments, Permutation Entropy is higher within the stable
 139 region than within ICH region and this difference is significant as Table 3
 140 shows no overlapping in the confidence intervals. Fig. 4 shows the histogram
 141 of the sampling distribution for the PE estimated over the ICH region and

| Patient | Age | Gender | Diagnosis | Length of stay(d) | Survival |
|------------------------------|-----|--------|-------------------------|-------------------|----------|
| 42210 | 42 | F | subarachnoid hemorrhage | 15 (h) | Y |
| 44789 | 67 | F | subarachnoid hemorrhage | 24 | Y |
| 51909 | 47 | M | subarachnoid hemorrhage | 16 | Y |
| 53639 | 47 | F | subarachnoid hemorrhage | 17 | Y |
| 59991 | 63 | M | subarachnoid hemorrhage | 34 | Y |
| 74438 | 33 | M | intracranial hemorrhage | 55 | Y |
| 79228 | 63 | M | intracranial hemorrhage | 27 | N |
| 85892 | 57 | F | intracranial hemorrhage | 19 | Y |
| 87913 | 60 | F | intracranial hemorrhage | 22 | Y |
| 87969 | 78 | F | intracranial hemorrhage | 82 | Y |
| 89002 | 41 | F | subarachnoid hemorrhage | 21 | Y |
| 95951 | 82 | F | intracranial hemorrhage | 9 | N |
| <i>mean ± sd</i> 56.9 ± 14.8 | | | | | |

Table 1: There were 9 females and 3 males with an age with a range from 32 to 82 years old and a mean of 56.9 ± 14.8 years old, the length of the stay in the ICU was from 9 to 82 days; six patients suffer for subarachnoid hemorrhage and six patients, intracranial hemorrhage and there were 2 nonsurvival patients.

| Segments | # ICH episodes | ICH summary | |
|----------|----------------|-------------|-----------|
| | | Mean(ICP) | Std (ICP) |
| 3365681 | 1 | 22.79 | 0.93 |
| 3487247 | 1 | 23.41 | 0.68 |
| 3629298 | 1 | 28.19 | 0.2615 |
| | | 22.97 | 2.80 |
| 368853 | 4 | 30.83 | 0.30 |
| | | 23.59 | 0.71 |
| | | 31.18 | 1.46 |

Table 2: Mean and standard deviation of the ICP within the patients segments for the ICH episodes.

142 stable region respectively. The sampling distribution approximation was ob-
 143 tained using the bootstrap proposed in [8].

144 Along with PE, the *Number of Missing Patterns* was calculated in the same
 145 way. Table 4 shows the NMP calculated over the stable region and the ICH
 146 for each patient along with its standard deviation, for all patient the dif-
 147 ference is statistically significant, in Fig. 5 the histogram of the sampling
 148 distribution for the NMP estimated over the ICH region and stable region
 149 is shown. Again, the sampling distribution of the NMP was approximated
 150 using the bootstrap proposed in [8].

151

| Segment | Stable | ICH |
|---------|--------------------|-----------------|
| 3365681 | 0.1736±0.0201 | 0.1597±0.0021 |
| 3487247 | 0.2249±0.0130 | 0.1783±0.0042 |
| 3629298 | - | 0.2615±0.003 |
| | 1 0.2293± 0.031 | 0.1743±0.0105 |
| | 2 0.2144 ± 0.01001 | 0.1757 ± 0.0091 |
| 3688532 | 3 0.2106 ± 0.0210 | 0.2062 ± 0.0035 |
| | 4 0.1957 ± 0.0205 | 0.1754 ± 0.0026 |

Table 3: *Permutation Entropy* of the Stable and Intracranial Hypertension (ICH) for all patients analyzed within this paper. Patient 85892 does not has a stable region. Across all segments, *Permutation Entropy* is higher within the stable region than within ICH region. Patient 74438 has suffered 4 ICH episodes.

152 3. Discussion

153 The concept of homeostasis in physiology implies that the system oper-
 154 ates in a stable state, or fixed point attractor, where the process fluctuates
 155 around a stable value. Then we can define a complex biological system as
 156 one that is very sensitive to small changes in initial conditions and reacts
 157 adaptively to minimal changes in its environment. Therefore, the complex-
 158 ity of such a system can directly correlate with its ability to react to change
 159 and, when this capacity is lost, we can postulate that the complexity of the
 160 system is also adversely affected. Therefore for these systems, it has been
 161 hypothesized that complexity decreases in the presence of a stressor [41].
 162 This is what we see in the Table 3 and in Fig. 4: periods of hypertension

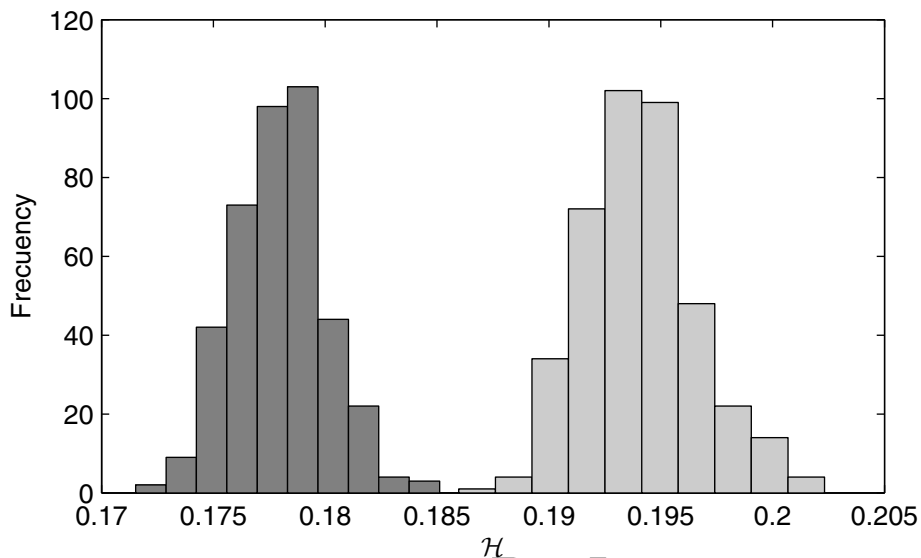


Figure 4: Histogram approximating the sampling distribution of the PE for the stable region (light gray) and the ICH region (dark gray) for the patient 87969. Note the statistically significant reduction in the PE calculated over the ICH region. The sampling distribution of PE was drawn using a bootstrap approach presented in [8].

| Segment | Stable | ICH |
|---------|--------------|--------------|
| 3365681 | 582 ± 12 | 672 ± 20 |
| 3487247 | 519 ± 15 | 580 ± 13 |
| 3629298 | - | 505 ± 11 |
| 1 | 541 ± 14 | 632 ± 15 |
| 2 | 671 ± 11 | 626 ± 17 |
| 3688532 | 605 ± 14 | 646 ± 15 |
| 4 | 489 ± 13 | 625 ± 12 |

Table 4: *Number of Missing Patterns* (NMP) of the stable region and Intracranial hypertension (ICH) for all patients analyzed within this paper. Patient 85892 does not have a stable region. Across all patients, the NMP is lower within the stable region than within the ICH region. Patient 74438 has suffered 4 ICH episodes.

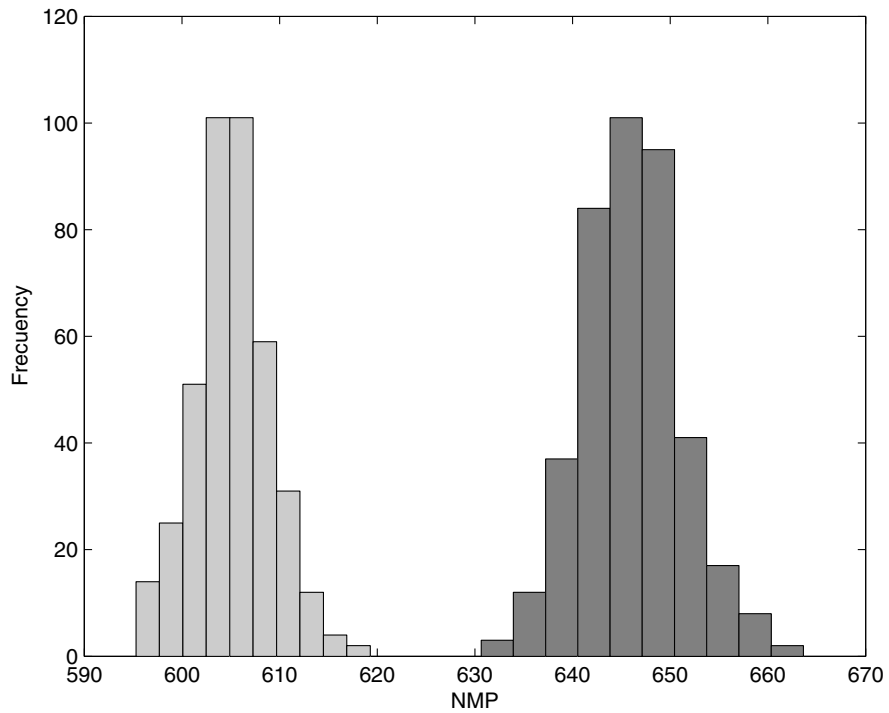


Figure 5: Histogram approximating the sampling distribution of the NMP for the stable region (light gray) and the ICH region (dark gray) for the patient 87969. Note the statistically significant reduction in the NMP calculated over the ICH region. The sampling distribution of NMP was drawn using a bootstrap approach presented in [8].

163 have a lower entropy than the stable period for each patient. The action of
164 the positive feedback (Rosners vasodilatory cascade), see Fig. 1, causes an
165 instability that when the three negative loops (escapes ways) are not able to
166 counteract this instability, a transition zone is presented and finally a new
167 metastable equilibrium is achieved with a lower complexity than the initial
168 state.

169 The state above indicates that a loss of complexity occurs within an hyper-
170 tension episode and the feedback loop model may lead to an explanation of
171 this loss. According to [41], the loss of complexity may reflect the loss or
172 impairment of functional components of the system, in this case when the
173 mechanism of cerebral auto-regulation exhausts, i.e. the negative loops, the
174 complexity of the ICP decreases and this fact is interesting because com-
175 plexity measured using the PE reflects a physiological fact and not just an
176 epiphenomena.

177 In Table 4, and in Figure 5 for patient 87969, there is an increase in the
178 number of missing patterns in the periods of hypertension regarding to the
179 stability stages. This seems to indicate a presence of lower degrees of freedom
180 in the system of the dynamics of the ICP signal that is observed during the
181 periods of ICH demonstrating a lower adaptability of the cerebrovascular sys-
182 tem. That is to say, the cerebrovascular system loses the capacity to respond
183 adequately due to the fact that its regulation mechanisms are diminished,
184 and therefore this system loses complexity, so it has a smaller spectrum of
185 possible responses and therefore less adaptability to stress. When losing the
186 ability to respond, secondary lesions may occur due to lack of adaptation to
187 changes in the environment such as blood pressure, temperature, etc. Our
188 results are concordant with those found by Hornero *et al.* [42] in a population
189 of *pediatric patients with traumatic brain injury* and, as *our population are*
190 *adult patients with strokes of different origins, this suggests that the decrease*
191 *in the complexity of the cerebrovascular system is independent of the type of*
192 *primary injury and age.*

193 From the point of view of the *clinical implication*, in Lu *et al.* [36] showed
194 that *the loss of the complexity of the intracranial pressure signal correlates*
195 *with worse outcomes. So we should ask if beyond the isolated value of in-*
196 *tracerebral pressure, we should not act on changes in the complexity of the*
197 *signal as it provides important information about the status of cerebral au-*
198 *toregulation and can be already determined in real time. Besides, this could*
199 *help us to generate therapies to decrease intracranial pressure and thus pro-*
200 *vide a greater spectrum of responses to avoid secondary damage to the lack*

201 *of regulation of the cerebrovascular system as discussed above.*

202 We are aware about some limitations of our study, the signals analyzed in
 203 this study came from 7 patient, and more patients should be sampled in
 204 order to empirically validate the mathematical model; we use an external
 205 database and we have no control about the clinical trial and the outcome
 206 recorded, and finally no direct or indirect measurements were performed in
 207 cerebral autoregulation. In summary, this article presents more evidence of
 208 the need of incorporating more information for the evaluation of the complete
 209 intracranial pressure signal than the usual waveform obtained by neuromon-
 210 itoring since these analysis provide us with fundamental information about
 211 the pathophysiological aspects of neurocritical patients and help us determine
 212 future interventions.

213 **Apendix I**

214 When computing the Shannon Entropy defined in Eq. 1 there are several
 215 ways to determine the π_i states. For example, if the histogram is used, once
 216 n bins are set, the possible states of the system $S = \pi_1, \dots, \pi_n$ are fixed and
 217 the times where the system is in the p_{ith} state are counted and its relative fre-
 218 quency (probability of appearance, i.e. $P(\pi_i)$), is computed and used in Eq.
 219 1 to quantify the Entropy. Although this method, i.e. using the histogram
 220 to determine the possible states and compute their relative frequency, can
 221 grasp the difference in the variance, symmetry and kurtosis of the probability
 222 distribution function (PDF) of the π_i states, it does not take account for the
 223 time dynamic of the system, and this fact can be an issue when a dynamical
 224 system, as Cerebral Autoregulation, is under study. One way to cope with
 225 this issue is by using the symbolization proposed by Bandt and Pompe (BP-
 226 symbolization) in [15] to determine the π_i states and therefore compute $P(\pi_i)$
 227 and Eq. 1. The BP-symbolization consists, from a practical point of view,
 228 in mapping the system evolution, given in form of time series, onto a set of
 229 symbols \mathcal{S}_m . To do that, two parameter must be fixed, the symbol length
 230 m , which is related with the information content of each symbol belonging
 231 the set \mathcal{S}_m (the higher the m value, the higher the informational content)
 232 and the time delay τ , related to temporal scales (within this article $\tau = 1$ to
 233 avoid temporal scale difficulties). Due to computational limitations, m goes
 234 usually $3 \leq m \leq 6$ and it is set as $m = 6$ within this article. Fig. 3 shows
 235 the BP-methodology to compute $P(\pi)$ for $m = 3$. The methodology simply
 236 maps each value x_i in the embedding vector $X_m(t) = \{x_t, \dots, x_{t+m-1}\}$ ordering

237 its index $t \in \{1, 2, \dots, m\}$ according to the increasing amplitude (rank) of
 238 each x_i in $X_m(t)$. It can be seen that the indexes of the time axis are fixed in
 239 chronological order, and they are mapped onto the vertical (amplitude) axis.
 240 For each pattern $X_3(t) = (x_t, x_{t+1}, x_{t+2})$, the resultant symbol $\pi_i \in S_3$ can be
 241 obtained reading the labels in the vertical axis from the bottom to the top
 242 (in the direction of the increasing amplitude). The higher the value of the
 243 Entropy computed using the BP-Methodology, the higher the uncertainty in
 244 the correlation structure of the time series and thus, higher the complexity.
 245 A related concept along with the BP-symbolization is the Number of Miss-
 246 ing Patterns (NMP). Once a time series is mapped onto a group \mathcal{S}_m some
 247 symbols π_i could have no occurrence and the corresponding $P(\pi_i) = 0$. If
 248 the time series is large enough and the time series has a stochastic nature,
 249 *NMP* has to be 0, otherwise, if the time series were deterministic, *NMP*
 250 may be greater than zero, i.e. *NMP* could be interpreted as a driver to detect
 251 determinism in a time series, provided a large enough time span. An inter-
 252 esting interpretation of the *NMP* is that their presence could be understood
 253 as the degree of freedom of the system, the higher the *NMP* the lower degree
 254 of freedom of the time series; e.g. a random time series has *NMP*=0 and in
 255 contrast a chaotic time series can have *NMP* ≥ 0 , no matter the time series
 256 span.

References

- [1] A. Bhatia, A. K. Gupta, Neuromonitoring in the intensive care unit. i. intracranial pressure and cerebral blood flow monitoring, *Intensive care medicine* 33 (2007) 1263–1271.
- [2] S. Neff, R. Subramaniam, Monro-kellie doctrine., *Journal of neurosurgery* 85 (1996) 1195–1195.
- [3] C. Avezaat, J. Van Eijndhoven, D. Wyper, Cerebrospinal fluid pulse pressure and intracranial volume-pressure relationships., *Journal of Neurology, Neurosurgery & Psychiatry* 42 (1979) 687–700.
- [4] M. Rosner, Cerebral perfusion pressure: link between intracranial pressure and systemic circulation, in: Wood (Ed.), *Cerebral Flood Flow: Physiologic and Clinical Aspects*, McGraw Hill, New York, N.Y., The address of the publisher, 1987, p. 42588.

- [5] M. Ursino, C. A. Lodi, A simple mathematical model of the interaction between intracranial pressure and cerebral hemodynamics, *Journal of Applied Physiology* 82 (1997) 1256–1269.
- [6] D. Kaplan, M. Furman, S. Pincus, S. Ryan, L. Lipsitz, A. Goldberger, Aging and the complexity of cardiovascular dynamics, *Biophysical Journal* 59 (1991) 945–949.
- [7] L. A. Lipsitz, A. L. Goldberger, Loss of ‘complexity’ and aging: Potential applications of fractals and chaos theory to senescence, *Jama* 267 (1992) 1806–1809.
- [8] F. Traversaro, F. Redelico, Confidence intervals and hypothesis testing for the permutation entropy with an application to epilepsy, arXiv preprint arXiv:1705.06732 (2017).
- [9] F. O. Redelico, F. Traversaro, M. d. C. García, W. Silva, O. A. Rosso, M. Risk, Classification of normal and pre-ictal eeg signals using permutation entropies and a generalized linear model as a classifier, *Entropy* 19 (2017) 72.
- [10] C. Bian, C. Qin, Q. D. Ma, Q. Shen, Modified permutation-entropy analysis of heartbeat dynamics, *Physical Review E* 85 (2012) 021906.
- [11] Y. Tuininga, D. Van Veldhuisen, J. Brouwer, J. Haaksma, H. Crijns, K. Lie, et al., Heart rate variability in left ventricular dysfunction and heart failure: effects and implications of drug treatment., *Heart* 72 (1994) 509–513.
- [12] M. Soehle, M. Czosnyka, D. A. Chatfield, A. Hoeft, A. Peña, Variability and fractal analysis of middle cerebral artery blood flow velocity and arterial blood pressure in subarachnoid hemorrhage, *Journal of Cerebral Blood Flow & Metabolism* 28 (2008) 64–73.
- [13] M. Gell-Mann, Simplicity and complexity in the description of nature, *Engineering and Science* 51 (1988) 2–9.
- [14] L. Tang, H. Lv, F. Yang, L. Yu, Complexity testing techniques for time series data: A comprehensive literature review, *Chaos, Solitons & Fractals* 81 (2015) 117–135.

- [15] C. Bandt, B. Pompe, Permutation entropy: a natural complexity measure for time series, *Physical review letters* 88 (2002) 174102.
- [16] R. M. Gray, *Entropy and information theory*, Springer Science & Business Media, 2011.
- [17] M. Riedl, A. Müller, N. Wessel, Practical considerations of permutation entropy, *The European Physical Journal Special Topics* 222 (2013) 249–262.
- [18] C. Quintero-Quiroz, S. Pigolotti, M. Torrent, C. Masoller, Numerical and experimental study of the effects of noise on the permutation entropy, *New Journal of Physics* 17 (2015) 093002.
- [19] F. Traversaro, R. F, Characterization of autoregressive processes using entropic quantifiers, *Physica A: Statistical Mechanics and its Applications* (2017).
- [20] N. Pariz, A. Karimpour, Fast and robust detection of epilepsy in noisy eeg signals using permutation entropy, *Bioinformatics and Bioengineering*, 2007. BIBE 2007 (2007).
- [21] D. Jordan, G. Stockmanns, E. F. Kochs, S. Pilge, G. Schneider, Electroencephalographic order pattern analysis for the separation of consciousness and unconsciousness: an analysis of approximate entropy, permutation entropy, recurrence rate, and phase coupling of order recurrence plots, *The Journal of the American Society of Anesthesiologists* 109 (2008) 1014–1022.
- [22] X. Li, S. Cui, L. J. Voss, Using permutation entropy to measure the electroencephalographic effects of sevoflurane, *Anesthesiology: The Journal of the American Society of Anesthesiologists* 109 (2008) 448–456.
- [23] E. Olofsen, J. Sleight, A. Dahan, Permutation entropy of the electroencephalogram: a measure of anaesthetic drug effect, *British journal of anaesthesia* 101 (2008) 810–821.
- [24] A. Silva, H. Cardoso-Cruz, F. Silva, V. Galhardo, L. Antunes, Comparison of anesthetic depth indexes based on thalamocortical local field potentials in rats, *Anesthesiology: The Journal of the American Society of Anesthesiologists* 112 (2010) 355–363.

- [25] A. Silva, S. Campos, J. Monteiro, C. Venâncio, B. Costa, P. G. de Pinho, L. Antunes, Performance of anesthetic depth indexes in rabbits under propofol anesthesia: prediction probabilities and concentration-effect relations, *The Journal of the American Society of Anesthesiologists* 115 (2011) 303–314.
- [26] D. Li, X. Li, Z. Liang, L. J. Voss, J. W. Sleight, Multiscale permutation entropy analysis of eeg recordings during sevoflurane anesthesia, *Journal of neural engineering* 7 (2010) 046010.
- [27] S. Schinkel, N. Marwan, J. Kurths, Order patterns recurrence plots in the analysis of erp data, *Cognitive neurodynamics* 1 (2007) 317–325.
- [28] S. Schinkel, N. Marwan, J. Kurths, Brain signal analysis based on recurrences, *Journal of Physiology-Paris* 103 (2009) 315–323.
- [29] N. Nicolaou, J. Georgiou, Permutation entropy: a new feature for brain-computer interfaces, in: *Biomedical Circuits and Systems Conference (BioCAS)*, 2010 IEEE, IEEE, pp. 49–52.
- [30] A. E. Johnson, T. J. Pollard, L. Shen, L.-w. H. Lehman, M. Feng, M. Ghassemi, B. Moody, P. Szolovits, L. A. Celi, R. G. Mark, Mimic-iii, a freely accessible critical care database, *Scientific data* 3 (2016).
- [31] J. Lee, D. J. Scott, M. Villarroel, G. D. Clifford, M. Saeed, R. G. Mark, Open-access MIMIC-II database for intensive care research, 2011.
- [32] A. L. Goldberger, L. A. N. Amaral, L. Glass, J. M. Hausdorff, P. C. Ivanov, R. G. Mark, J. E. Mietus, G. B. Moody, C.-K. Peng, H. E. Stanley, PhysioBank, PhysioToolkit, and PhysioNet: Components of a new research resource for complex physiologic signals, *Circulation* 101 (2000 (June 13)) e215–e220.
- [33] G. B. Moody, R. G. Mark, A. L. Goldberger, Physionet: a web-based resource for the study of physiologic signals, *IEEE Engineering in Medicine and Biology Magazine* 20 (2001) 70–75.
- [34] D. J. Scott, J. Lee, I. Silva, S. Park, G. B. Moody, L. A. Celi, R. G. Mark, Accessing the public mimic-ii intensive care relational database for clinical research, *BMC Medical Informatics and Decision Making* 13 (2013) 9.

- [35] Y.-L. Huang, T. Badrick, Z.-D. Hu, Using freely accessible databases for laboratory medicine research: experience with mimic database, *Journal of Laboratory and Precision Medicine* 2 (2017).
- [36] C.-W. Lu, M. Czosnyka, J.-S. Shieh, A. Smielewska, J. D. Pickard, P. Smielewski, Complexity of intracranial pressure correlates with outcome after traumatic brain injury, *Brain* 135 (2012) 2399–2408.
- [37] M. J, C. C, B. J, A. M, E. M, L. S, G. B, Sensitive precursors to acute episodes of intracranial hypertension, *Proceedings of the 4th International Workshop in Biosignal* (2002).
- [38] J. McNames, C. Crespo, M. Aboy, M. Ellenby, S. Lai, R. Sciabassi, B. Goldstein, Precursors to rapid elevations in intracranial pressure, volume 4, 2001.
- [39] H. Roberto, A. Mateo, A. Daniel, M. James, W. Wayne, G. B. B, Complex analysis of intracranial hypertension using approximate entropy*, *Critical Care Medicine* 34 (2006).
- [40] C. E. Shannon, A mathematical theory of communication, *ACM SIG-MOBILE Mobile Computing and Communications Review* 5 (2001) 3–55.
- [41] D. E. Vaillancourt, K. M. Newell, Changing complexity in human behavior and physiology through aging and disease, *Neurobiology of aging* 23 (2002) 1–11.
- [42] R. Hornero, M. Aboy, D. Abasolo, J. McNames, W. Wakeland, B. Goldstein, Complex analysis of intracranial hypertension using approximate entropy, *Critical care medicine* 34 (2006) 87–95.